(Preprint) AAS 21-592

ECLIPSE MITIGATION STRATEGIES IN P/2 LUNAR RESONANT ORBITS

Paul Levinson-Muth*, Andres Dono†, Laura Plice‡

Lunar resonant orbits present several important challenges in terms of trajectory design, insertion, stability and eclipse mitigation. For some mission concepts, the placement of the initial orbital elements is fundamental to overcoming show-stopping performance values such as eclipse duration and orbit lifetime. Lunar resonant orbits need to maintain specific alignments in order to avoid undesired flybys or even recontact with Earth or GEO satellites. This paper presents methods to mitigate long eclipses while preserving achievable lunar resonant orbits that persist in the long term.

INTRODUCTION

The orbital period of a lunar resonant orbit (LRO) corresponds to a fraction of the period of the Moon's orbit around the Earth. High altitude and even moderately eccentric orbits in the Earth-Moon system rely on this phenomenon to avoid undesired lunar encounters that would alter the stability over time.

Several missions have achieved lunar resonance in the past; including IBEX with a P/3 lunar resonance[1] and TESS with a P/2 resonance[2] as well as the Arcus proposal with a P/4 mission[3,4]. More recent concepts such as the HelioSwarm NASA MIDEX proposal[3] have designed P/2 LROs, building upon the strategies TESS used to mitigate eclipses. The HelioSwarm concept includes the deployment of a swarm of small satellites that do not have the capability to maintain power during long umbra transits.

The Arcus orbit designers[3] noted an advantage of a P/4 science orbit that the maximum hypothetical Earth shadow with apogee in the ecliptic plane sets an upper bound for the design space. In the case of Arcus' 6.8-day period and eccentricity of roughly 0.49, the worst case of a 4.5 hour eclipse was within tolerance for the spacecraft, so no further design effort addressed eclipse mitigation.

In this paper, we focus on P/2 LROs. The slow apogee speeds of eccentric P/2 LROs make them susceptible to long eclipses[4], especially if they lie in the ecliptic plane (there is no standard definition of what constitutes a long eclipse; in this paper we will define a long eclipse as an eclipse lasting longer than 3 hours). We present several eclipse mitigation strategies for such orbits. We

* Flight Dynamics Analyst, Millennium Engineering and Integration Co., NASA Ames Research Center, Moffett Field, CA 94035.
† Flight Dynamics Lead, Millennium Engineering and Integration Co., NASA Ames Research Center, Moffett Field, CA 94035.
‡ Flight Dynamics Analyst, Metis Technology Solutions, NASA Ames Research Center, Moffett Field, CA 94035.

focus on Earth eclipses; lunar eclipses in P/2 LROs are possible, but they tend to have shorter durations and occur less frequently than Earth eclipses[5].

We mainly focus on P/2 LROs with eccentricities between 0.6 and 0.7; this range of eccentricities presents several advantages. First, this places apogee near the Moon's radius, which allows the option of a lunar swingby with moderate post-swingby delta-v costs to reach the designated orbit[6]. Second, it places the perigee radius on the order of 85,000 km, low enough to facilitate convenient data downlink and high enough to remain clear of the outer Van Allen belt.

The trajectory design efforts for TESS and HelioSwarm provide case studies for eclipse mitigation in P/2 LROs. TESS mitigated eclipses by selecting ecliptic inclination and argument of perigee values which kept the line of apsides out of the ecliptic plane[2,7]. HelioSwarm employs similar strategies.

METHOD

The Earth orbits the Sun in the ecliptic plane. An Earth-orbiting satellite only undergoes Earth eclipses when crossing the ecliptic plane, a fact leveraged by each of the eclipse mitigation strategies presented here. The first strategy reduces the frequency and duration of eclipses by selecting favorable ecliptic inclination (i_e) values, which in turn reduces the amount of time the satellite spends near the ecliptic plane. The second strategy rotates the line of apsides away from the ecliptic plane by selecting favorable ecliptic argument of perigee (ω_e) values, thereby keeping slow apogee speeds away from the ecliptic plane. The third strategy uses maneuvers to change the orbit period, shifting the timing of ecliptic crossings to avoid long umbra transits.

Except where noted, we use a full-force model (Earth gravity harmonics, lunar and solar gravity perturbations, SRP) to propagate the trajectories in this paper. We establish operationally stable lunar resonance by setting the Moon-Earth-satellite angle to 0° or 180° when the satellite is at perigee; this results in near-ideal lunar resonant alignment, well within the 30° lunar alignment requirement established by the TESS trajectory designers[7].

ECLIPTIC PLANE

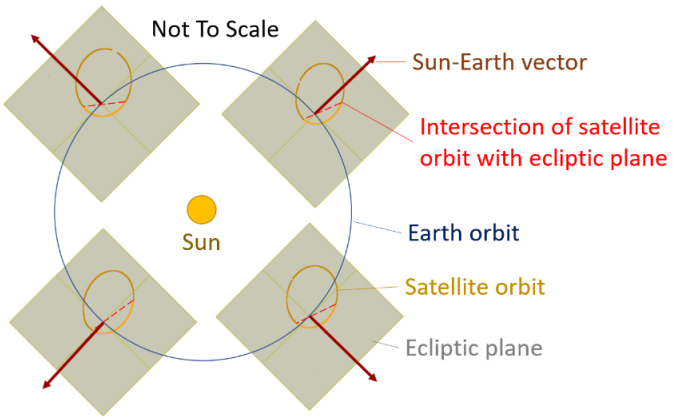


Figure 1. Illustration of ecliptic plane geometry. As the Earth orbits the Sun, the Sun-Earth vector sweeps through 360°; by comparison, the orientation of the satellite orbit relative to the ecliptic plane remains nearly fixed. Note that the intersection of the satellite orbit with the orbit plane is shown as an example only; the orientation of this intersection would vary for different orbit geometries.

The ecliptic plane provides a useful geometric framework for eclipse mitigation strategies. Earth eclipses occur when the Sun-Earth vector nearly aligns with the Earth-satellite vector; by definition,

this occurs near the intersection of the satellite's orbit plane with the ecliptic plane. Each year, the Sun-Earth vector sweeps through 360° in the ecliptic plane; compared to that rate, the orientation of the intersection of the satellite orbit plane with the ecliptic plane remains nearly fixed, as illustrated in Figure 1. This means that a favorable ecliptic orientation can help mitigate eclipses for years. i_e and ω_e provide powerful tools for designing the orientation of a satellite's orbit with respect to the ecliptic plane. We do not discuss ecliptic RAAN as a tool for eclipse mitigation in this paper; as the Sun-Earth vector sweeps through 360° in the ecliptic plane, it passes through every orbit plane regardless of ecliptic RAAN.

Ecliptic Inclination

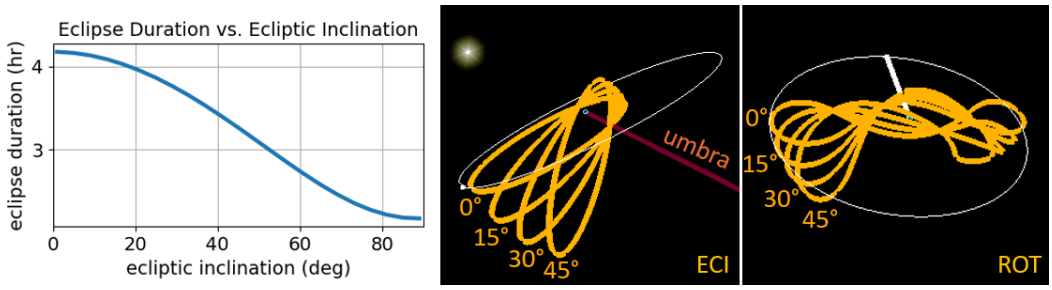


Figure 2. Eclipse duration as a function of ecliptic inclination. The plot on the left shows eclipse duration for an example ecliptic crossing. The center plot shows a selection of trajectories in the ECI frame with ecliptic inclination labeled; all other ecliptic parameters were held constant, resulting in comparable orientation relative to the Sun-Earth system. The plot on the right shows sample trajectories in the Earth-Moon rotating system; apogees remain far from the Moon, resulting in viable long-term resonance for all sampled inclinations.

Values of i_e can significantly affect eclipse duration for P/2 lunar resonant orbits, as illustrated by the following example. For an example P/2 lunar resonant orbit with a semi-major axis of 245,000 km, an eccentricity of 0.64, and an ω_e of 128˚, i_e determines the speed of ecliptic plane crossing, as shown in Figure 2. Larger i_e values result in faster ecliptic plane crossings: i_e values of 90° result in the fastest possible ecliptic crossing, while i_e values of 0° result in a trajectory that never leaves the ecliptic plane. Higher i_e values reduce time spent near the ecliptic plane, thereby reducing eclipse duration.

The advantages of shortening eclipse durations with high i_e values may be offset by other trajectory design considerations. Equatorial inclination can differ from ecliptic inclination by as little as 15° or as much as 60°, and mission constraints on equatorial inclination may derive from factors such as ground station visibility or launch opportunities. Transfer trajectories to LRO may use lunar gravity assist techniques, thereby allowing affordable plane changes, but adding complexity to the establishment of the mission orbit.

Ecliptic Argument of Perigee

As with i_e, the ω_e of a trajectory affects the timing of ecliptic crossings. The high eccentricities of most real-world P/2 LROs result in large differences in velocity between apogee and perigee. A satellite crosses the ecliptic plane twice per orbit; for an orbit with all other parameters fixed, the ω_e value determines the speed of each ecliptic crossing. An ω_e of 90° or 270° results in a pair of ecliptic crossings with equal speeds, while an ω_e of 0° or 180° results in the slowest possible ecliptic crossing at apogee and the fastest possible ecliptic crossing at perigee. This difference in ecliptic crossing speeds results in a difference in eclipse durations. As Figure 3 shows, eclipse durations peak when ω_e causes an ecliptic crossing near apogee.

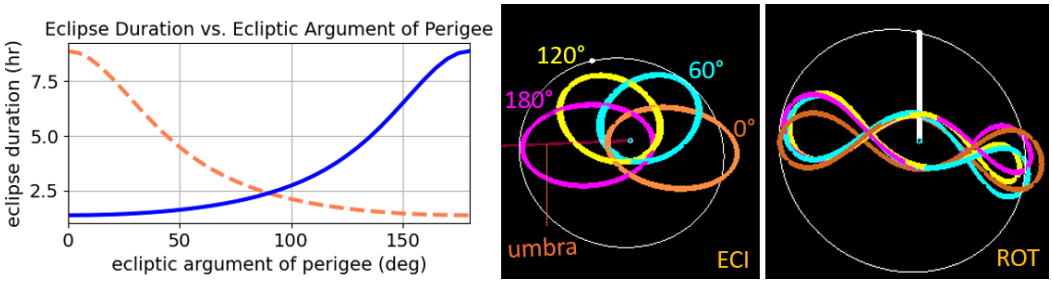


Figure 3. Eclipse duration as a function of ω_e. The blue line in the plot on the left shows eclipse duration as a function of ω_e for an example ecliptic crossing. The RAAN, true anomaly, and epoch of each sampled case were adjusted to ensure worst-case eclipse conditions and stable P/2 lunar resonance, ensuring consistency in the comparison. Note the Earth's rotation about the Sun means that the trend of worst-case eclipse durations will reflect roughly six months later, as shown by the orange dotted line.

It is important to note that the low eclipse durations shown for ω_e values near 0° do not represent long-term safety from eclipses; as the Earth rotates about the Sun, the umbra sweeps in a circle relative to the nearly inertially-fixed orbit, approaching the apogee of the $\omega_e = 0°$ orbit 6 months later. For that reason, ω_e values near 90° or 270° provide the best long-term eclipse mitigation.

Combined Effects of Ecliptic Parameters

Depending on the geometry of a given ecliptic crossing, the combined effects of i_e and ω_e on eclipse duration may vary. For example, Figure 4 shows that ω_e has a much stronger effect than i_e on eclipse duration for worst-case ecliptic crossings (that is, cases in which the Sun-Earth and Earth-satellite vectors align at the epoch of the ecliptic crossing). These cases are unusual, though. The Sun-Earth vector sweeps through 360° per year in the ecliptic plane; compared to that rate of motion, the intersection of a P/2 LRO with the ecliptic plane remains almost fixed. This means that the Sun-Earth vector sweeps through about 13.5° during the roughly 13.7 days that pass between two consecutive far-side ecliptic crossings of a P/2 LRO. It is possible to design P/2 LROs which spend years avoiding the worst-case geometry shown in Figure 4.

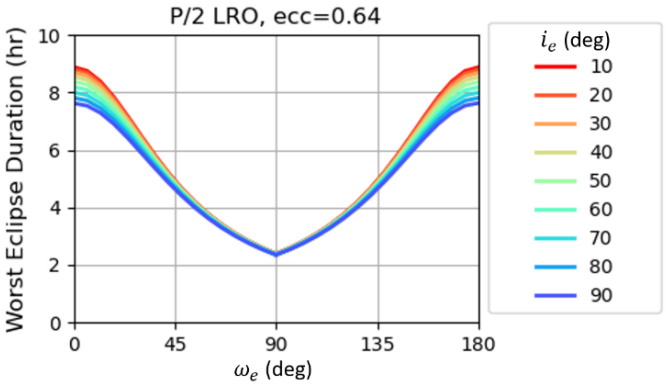


Figure 4. Worst-case eclipse duration as a function of ω_e and i_e. The semi-major axis and eccentricity were kept fixed; worst-case eclipse geometry was established by varying ecliptic RAAN and true anomaly such that the Sun-Earth vector aligned with the Earth-satellite vector at the time of ecliptic crossing; the epoch of ecliptic crossing was varied to ensure that the P/2 LRO maintained viable lunar resonant alignment. Cases were propagated in a full-force model.

Note that Figure 4 presents worst-case alignments for P/2 LROs with a fixed eccentricity of 0.64; as noted in the introduction, eccentricities near this magnitude result in an especially useful

class of P/2 LROs. A similar figure in Gangestad et al. (2013)[6] varies perigee radius instead of i_e, providing an excellent resource to understand the trade space for P/2 LROs over a wide range of eccentricities.

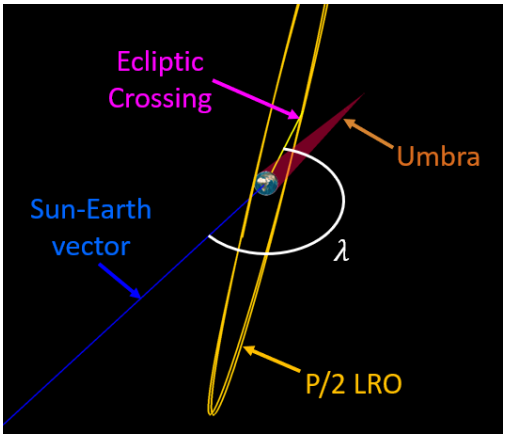


Figure 5. Example illustrating the Sun-Earth-ecliptic crossing angle (λ). The image corresponds to the epoch of the satellite's ecliptic crossing. In this example, λ has a value of 185°.

Because the effect of i_e is negligible for some ecliptic crossing geometries and relevant at others, we will use the Sun-Earth-ecliptic crossing angle to help quantify the parametric relationship between i_e, ω_e, and eclipse duration. We define the Sun-Earth-ecliptic crossing angle (λ) as the dihedral angle between the Earth-Sun and Earth-satellite vector measured about the ecliptic z-axis at the time of the satellite's ecliptic crossing; Figure 5 illustrates this geometry.

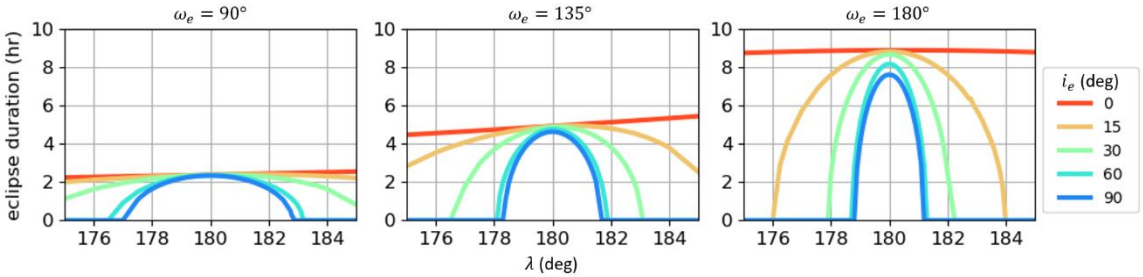


Figure 6. Eclipse duration as a function of λ for various i_e and ω_e values. These plots correspond to P/2 LROs with an eccentricity of 0.64.

As Figure 6 illustrates, λ has a significant effect on the relationship between i_e, ω_e, and eclipse duration. Values of λ near 180° correspond to worst-case or near-worst-case eclipses; in these configurations, i_e has a negligible effect on eclipse duration, with ω_e having the much stronger effects shown in Figure 4. For λ values a few degrees above or below 180°, i_e begins to have a much stronger effect, with higher i_e values reducing or eliminating eclipses. Importantly, i_e has a stronger mitigation effect at ω_e values near 180 and 0°; in other words, as the eclipse mitigation effects of ω_e decrease in strength, the mitigation effects of i_e increase in strength.

Each graph in Figure 6 details the satellite's crossing of the ecliptic plane near the anti-Sun alignment. Values of ω_e near 90° provide the strongest eclipse mitigation across the range of λ values; however, some missions may find it impractical to reach or maintain ω_e near this value. In those cases, i_e provides an alternative tool for mitigating eclipses, providing a large reduction in eclipse durations for all but the worst values of λ. In practice, a combination of high i_e values and ω_e values near 90° or 270° provides the best long-term eclipse mitigation.

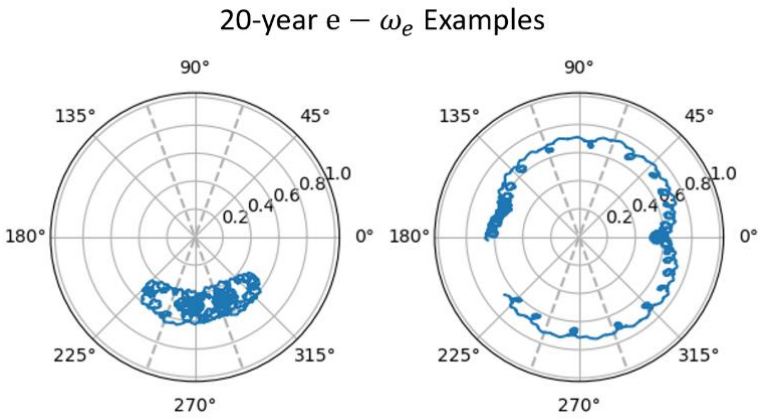


Figure 7. 20-year $e - \omega_e$ plots for two example P/2 LROs. In the case shown on the left, ω_e librates around 270°; in the case on the right, ω_e circulates and will eventually pass through 360°.

The perturbations affecting P/2 LROs tend to cause i_e and ω_e to evolve and precess. Though not the focus of this paper, it is useful to understand these effects when selecting ecliptic parameters for eclipse mitigation. In a P/2 lunar resonant orbit, the argument of perigee with respect to the Moon's orbit plane will either librate about 90° or circulate through all 360°, depending on the LRO's inclination relative to the Moon's orbit plane[6,8]. Here our focus is on ecliptic parameters. The Moon's orbit plane is only slightly (~5°) inclined relative to the ecliptic plane[9], so ecliptic parameters tend to follow the same trends as lunar-relative parameters, librating or circulating as shown in Figure 7. For some missions, it may not be practical to establish a high i_e or to maintain an ω_e near 90°. Depending on mission requirements, trajectory designers can use i_e, ω_e, or a combination of both to mitigate long eclipses.

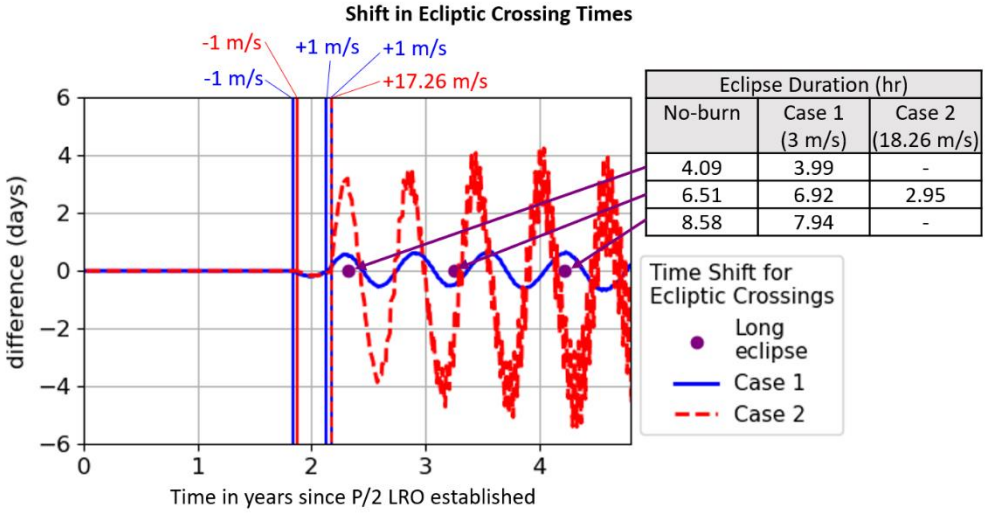
ECLIPSE PHASING MANEUVERS

A P/2 LRO crosses the ecliptic plane twice every 13.7 days, with a near-side crossing nearer to the Sun, and a far-side crossing further from the Sun. As we have seen, Earth eclipses take place when a satellite's far-side ecliptic crossing occurs at or near the same time the Sun-Earth vector crosses the satellite's orbit plane. The duration of the eclipse depends on how closely these crossings align; if the umbra-orbit plane crossing aligns exactly with one of the satellite's far-side ecliptic crossings (i.e. $\lambda \cong 180°$), a worst-case eclipse will occur, whereas if the umbra-orbit plane crossing occurs between two far-side ecliptic crossings (e.g. $\lambda_1 \cong 173.25°$, $\lambda_2 \cong 186.75°$), two short-duration eclipses may occur, or no eclipse at all.

By performing along-track maneuvers, a satellite can adjust its orbit period, altering λ by shifting the timing of ecliptic plane crossings. These shifts in ecliptic plane crossing times can reduce eclipse durations; however, lunar resonance tends to counteract shifts in timing. In a 2-body orbit the time shift would accumulate linearly with time, but in a P/2 LRO the orbit period oscillates about ~13.7 days, causing the time shift to oscillate about the no-burn timing. Figure 8 illustrates this oscillatory behavior for an example P/2 LRO, showing the shift in ecliptic crossing times for two example mitigation cases with respect to a reference case.

We have explored several cases spanning a range of delta-v capabilities. With three small maneuvers of 1 m/s each it is possible to reduce eclipse duration by at least 2.5%. The first mitigation maneuver initiates the time-shift oscillations, and the second and third mitigation maneuvers increase the amplitude. Larger delta-v capabilities allow greater reduction in eclipse duration. In our example case, a pair of maneuvers totaling 18.26 m/s reduces the second long eclipse by 55% and

completely eliminates the first and third long eclipses; however, there are several challenges when using maneuvers to mitigate eclipses.



Eclipse Duration (hr)		
No-burn	Case 1 (3 m/s)	Case 2 (18.26 m/s)
4.09	3.99	-
6.51	6.92	2.95
8.58	7.94	-

Figure 8. Shift in ecliptic crossing times for mitigation maneuver cases compared to a reference trajectory with no maneuvers. Mitigation maneuvers occur at the times indicated by the vertical lines, and all maneuvers occur in the velocity direction at perigee. Note that the initial maneuver occurs one perigee earlier for case 1 than for case 2 in order to maximize each case's ecliptic crossing time shift at the first long eclipse epoch.

Figure 9 shows the evolution of orbit period and eccentricity for the example cases from Figure 8. The orbit periods of all three cases oscillate about an average value of roughly 13.7 days, corresponding to roughly half the Moon's orbit period. The larger mitigation maneuver set induces larger amplitude oscillations in orbit period. The eccentricities also tend to oscillate, and the average eccentricity value drifts slightly for all three cases.

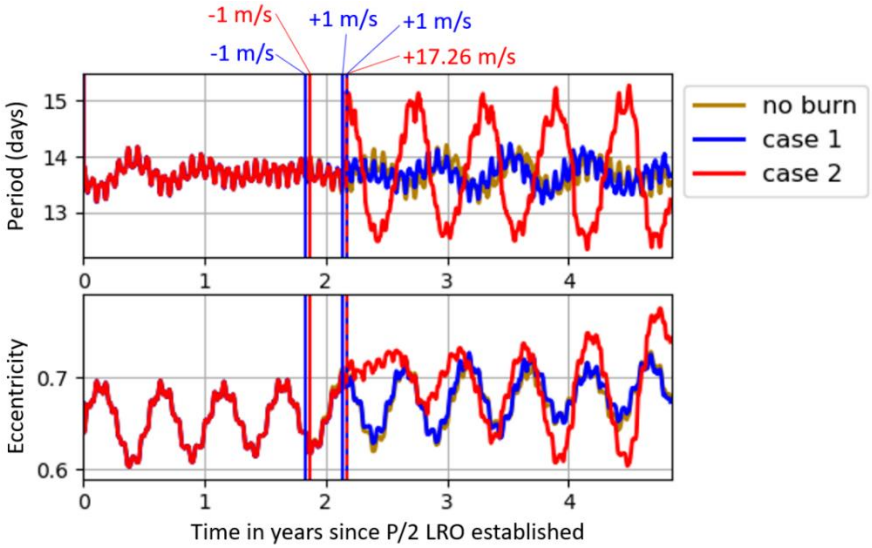


Figure 9. Evolution of orbit period and eccentricity for mitigation maneuver cases and a reference trajectory with no maneuvers. Mitigation maneuvers occur at the times indicated by the vertical lines, and all maneuvers occur in the velocity direction at perigee.

Larger mitigation maneuvers may induce greater shifts away from the ideal lunar resonant alignment. Missions utilizing LROs typically attempt to place apogee as far from the Moon as possible in order to reduce lunar perturbations and avoid unwanted lunar encounters[7,10]; for P/2 LROs, this means placing the Moon-Earth-apogee angle near 90° and 270°. The eclipse mitigation maneuvers explored here function by altering the orbit period, which changes the orientation of the LRO apogee with respect to the Moon. P/2 LROs can tolerate some deviation from the ideal alignment, and will oscillate about the ideal alignment if the offset is small enough; however, mission designers should consider this effect when planning maneuvers which will alter the orbit period of a P/2 LRO. Figure 10 illustrates this phenomenon for our example P/2 LRO; larger mitigation maneuvers tend to result in greater disruptions to the lunar resonant alignment.

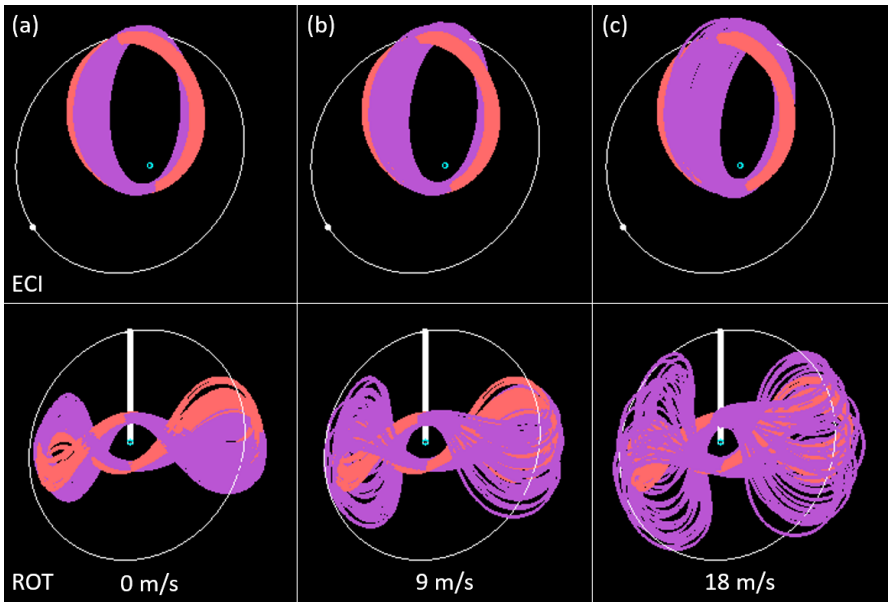


Figure 10. Trajectories shown in the ECI and Earth-Moon rotating frames, with varying magnitudes of mitigation maneuvers. Column (a) shows the trajectory with no mitigation burns, column (b) shows the trajectory with a pair of maneuvers totaling 9 m/s, and column (c) shows the trajectory with a pair of maneuvers totaling 18 m/s. The salmon color shows the pre-maneuver trajectory, extending roughly 2 years; the purple color shows the post-maneuver trajectory, extending roughly 2.8 years. Larger mitigation maneuvers tend to push the P/2 LRO further away from ideal resonant alignment.

A set of maneuvers that reduces the duration of one eclipse may increase the duration of a later eclipse. Plots in the style of the eclipse profile plot presented in Parker et al. (2018)[11] provide a powerful tool for analyzing the effects of a set of maneuvers on multiple eclipses. Figure 11 shows a profile of eclipse durations vs. time for varying mitigation maneuver magnitudes. As the maneuver magnitude increases from roughly 0 to 14 m/s, the duration of the first long eclipse (occurring at ~2.2 years) decreases, but the duration of the second long eclipse (occurring at ~3.2 years) increases. For maneuver magnitudes from roughly 12 to 16 m/s, the magnitude of the third long eclipse (occurring at ~4.2 years) increases. It is not until the maneuver set magnitude reaches 18.26 m/s that all three long eclipse durations fall below 3 hours. Eclipse mitigation using maneuvers requires this type of holistic approach to understand the effect of a maneuver set on all eclipses within the time of interest.

Figure 10 offers some useful options to the mission designer. Taking a use case with a primary mission duration of two years in orbit, there are eclipse concerns for the extended mission out to 5 years. Time on the x-axis is the same for all versions of the mission and naturally the eclipse

durations designed for relatively short durations in early mission years are the throughout the nominal mission. In the extended mission use case, there are concerns for eclipse duration at 2.3 years, 3.2 years, and 4.2 years, while the eclipses at the opposite time of year (2.9, 3.8, and 4.8 years) are short in all cases. The mission designer with constraints on mission duration and propellant may wish to prioritize the earliest post-maneuver eclipse and reduce its duration from 5 hours to 3 hours with a 14 m/s second maneuver. If delta-v and orbit evolution effects allow, then a larger second maneuver of 20 m/s can clear all of the longest eclipses for the 5 year case.

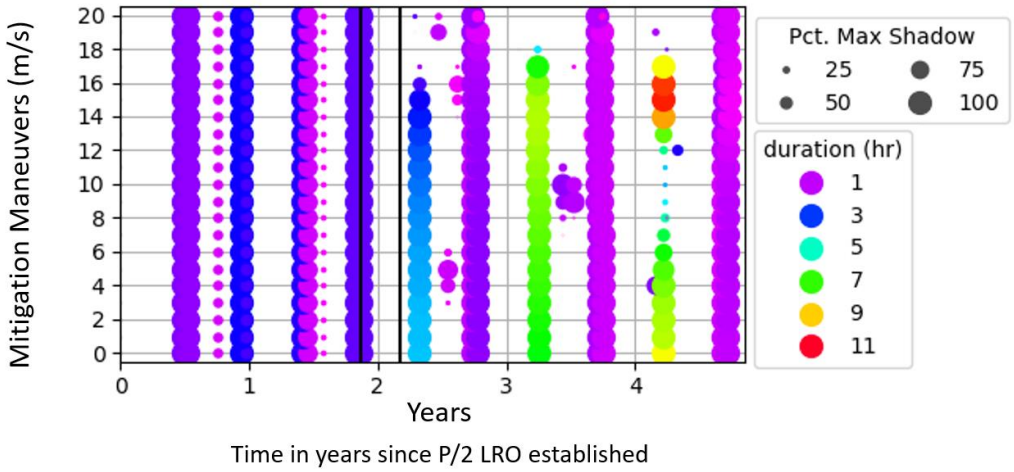


Figure 11. Eclipse durations and percentages vs. time and mitigation maneuver magnitude for an example P/2 LRO. The mitigation maneuvers occur at the times marked with vertical black lines; except in the 0 m/s case, the first maneuver has magnitude 1 m/s in the anti-velocity direction, and the second maneuver has the remainder of the magnitude shown in the ordinate in the positive velocity direction; in the 0 m/s case, both maneuvers have zero magnitude. All maneuvers occur at perigee, and the maneuvers occur at the same time in all cases.

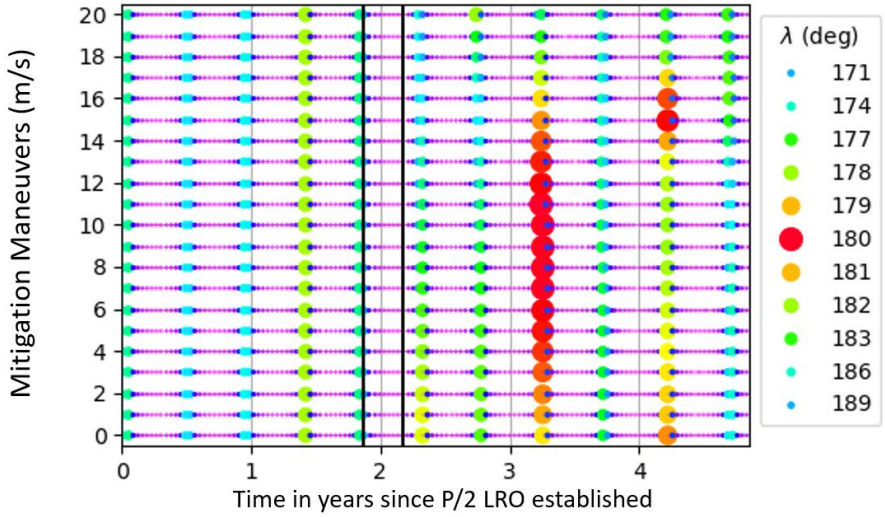


Figure 12. Ecliptic crossings vs. time and mitigation maneuver magnitude for the same example P/2 LRO shown in Figure 11. Most crossings do not present a risk of eclipse; large points with color scheme shown indicate λ values which may result in an Earth eclipse. Mitigation maneuvers occur at the times indicated by the vertical black lines.

The trends shown in Figure 11 arise primarily from shifts in λ, though altering λ does not always reduce eclipse durations; if λ shifts closer to 180°, eclipse durations will typically increase. Figure 12 shows a profile of λ values for the same P/2 LRO example; a comparison of the two figures reveals that maximum eclipse durations occur when λ is near 180°, as expected.

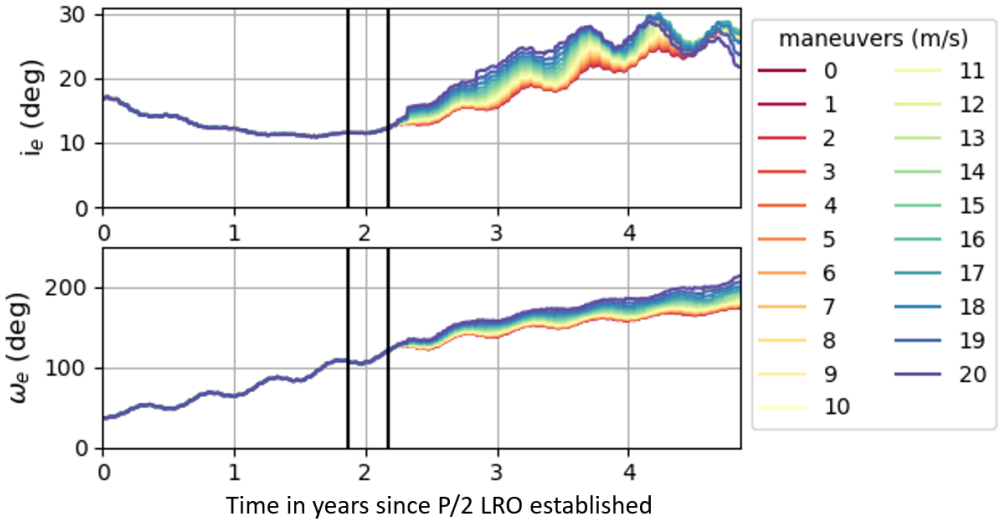


Figure 13. Variations in i_e and ω_e for various mitigation maneuver magnitudes. Mitigation maneuvers occur at the times indicated by the vertical black lines.

Mitigation maneuvers also result in slight variations of i_e and ω_e, but the magnitude of these changes have a small effect on eclipse duration compared to the effects of the λ shifts. Figure 13 shows i_e and ω_e trends for varying maneuver set magnitudes.

MISSION DESIGN APPLICATIONS

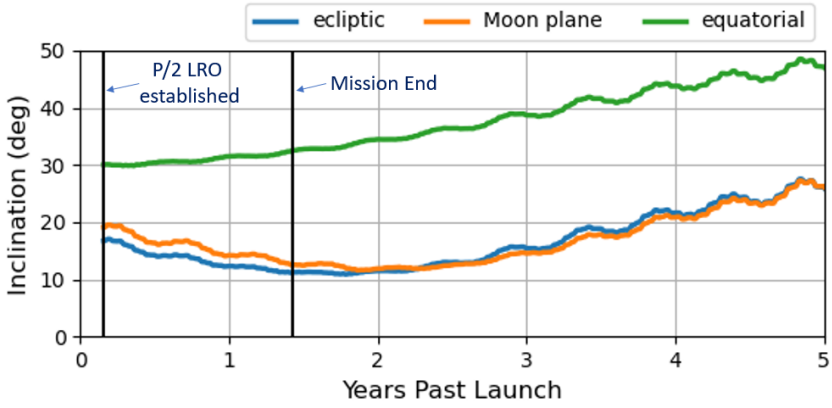


Figure 14. 5-year inclination trends for the HelioSwarm baseline trajectory. The plot includes inclinations with respect to the ecliptic plane, Moon's orbit plane, and equatorial plane. Note that the 18-month mission ends where indicated.

The trajectory design effort for the HelioSwarm mission concept, currently in Phase A MIDEX competition in NASA's Science Mission Directorate 2018 Heliophysics announcement, provides a case study for eclipse mitigation in a P/2 LRO. The HelioSwarm mission concept involves using phasing loops and a lunar swingby to reach a P/2 LRO with an eccentricity of approximately 0.65. After reaching the P/2 LRO, 8 "node" spacecraft will separate from the central "hub" spacecraft,

establishing relative trajectories to enable simultaneous multiscale measurements of the solar wind[5]. The small node spacecraft have limited power storage capabilities, necessitating mitigation of long (>3 hour) eclipses during the 18-month mission. In addition, the i_e value of the P/2 LRO must remain under 30° during the mission to facilitate observation of the solar wind across the desired scales.

As Figure 14 illustrates, i_e remains between roughly 11° to 17° during the baseline HelioSwarm mission, and the inclination with respect to the Moon's orbit plane follows roughly the same trend as i_e. For inclinations this low, ω_e will typically circulate[6], eventually passing through all 360° as illustrated by the right-hand plot in Figure 7. For this reason, HelioSwarm selects a set of initial conditions for the P/2 LRO such that ω_e will evolve through a favorable range of values over the course of the mission. The P/2 LRO's ω_e starts with a value of roughly 36° and evolves to a value of 86° by the end of the mission, as shown in Figure 15.

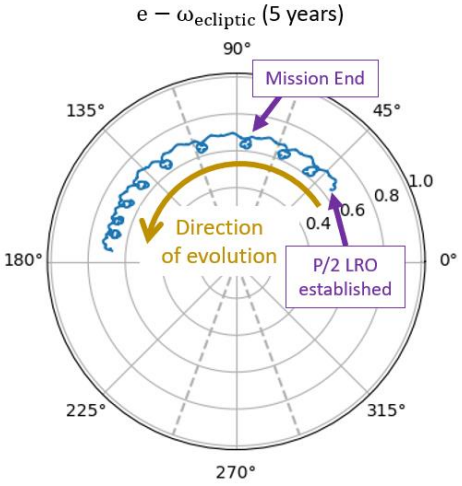


Figure 15. 5-year $e - \omega_e$ plot for the HelioSwarm baseline trajectory. Note that the 18-month mission ends where indicated.

HelioSwarm carries a 3-hour constraint on eclipse duration during the 12 month Science Phase, and an even tighter 2-hour eclipse constraint prior to the start of the Science Phase; eclipse mitigation strategies prior to the establishment of the P/2 LRO are beyond the scope of this paper. By setting ω_e within a favorable range, HelioSwarm keeps eclipse durations under 3 hours during the Science Phase, as shown in Figure 16.

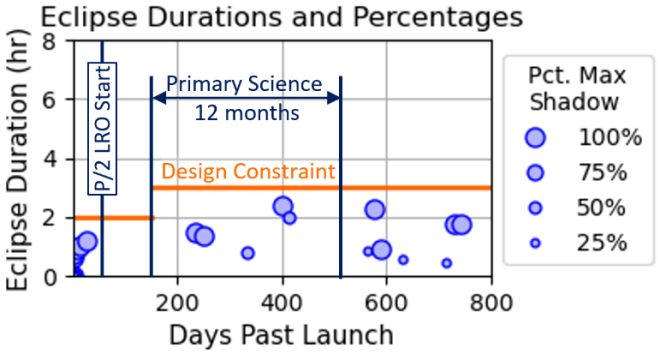


Figure 16. Eclipse durations and percentages for the HelioSwarm baseline trajectory. The 2- and 3-hour constraints on eclipse duration are shown in red.

For ω_e values from roughly 74° to 106°, even the theoretical worst-case geometry shown in Figure 4 results in eclipse durations under 3 hours. HelioSwarm avoids worst-case λ values while ω_e is lower than 74°, and the range of i_e is high enough to meet the eclipse constraints. Figure 17 shows a profile of λ vs. time for the HelioSwarm baseline trajectory; during the 18-month mission, the worst-aligned ecliptic crossing has a λ of 175°. Phase A analyses indicate an ability to meet eclipse requirements for the full range of expected launch energy dispersions.

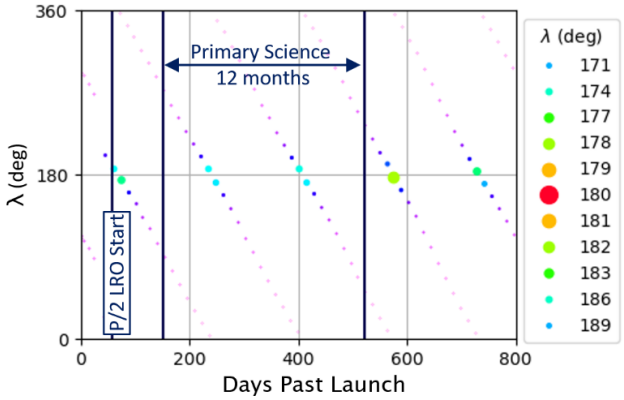


Figure 17. Profile of λ vs. time for the HelioSwarm baseline trajectory. Values of λ near 180° are indicated by larger markers with the color scheme shown in the legend.

HelioSwarm's short mission duration, coupled with the requirement that its i_e value remain below 30°, inform its eclipse mitigation strategy. Other missions utilizing P/2 LROs may face different sets of constraints, but HelioSwarm's experience exemplifies the type of considerations that often drive trajectory design. The strategies presented in this paper provide mission designers with multiple tools for mitigating eclipses; our hope is that these tools can prove useful for a broad set of missions.

FUTURE WORK

In this paper, we focus on techniques to mitigate Earth eclipses for P/2 lunar resonant orbits, and we limit our phasing maneuver investigation to impulsive maneuvers at apogee or perigee. Future work includes addressing strategies to mitigate Moon eclipses, exploring alternative placements for impulsive phasing maneuvers, and investigating the use of low thrust maneuvers to mitigate eclipses. A method to efficiently shift λ without disrupting the lunar resonant alignment would be especially useful.

CONCLUSION

Lunar resonant orbits are especially important due to the advantage of having high eccentricity and altitude in the Earth-Moon system while maintaining stability. Spacecraft missions in this environment face several challenges, including long term stability and eclipses. This paper presents methods and strategies to minimize the likelihood and duration of these eclipses while preserving the stability of the orbit. The first two methods include the application of fundamental principles of orbital mechanics by selecting favorable ecliptic inclination and argument of perigee values, while the third method uses maneuvers to alter the timing of ecliptic crossings.

ACKNOWLEDGMENTS

The authors of this paper would like to thank the sponsorship from the Spaceflight Division at NASA Ames Research Center and the HelioSwarm mission team for their continuous feedback and

support. Thank you to Dr. Kira Abercromby for years of guidance and support in and out of the classroom. As always, enduring gratitude goes to the late Professor Harm Buning, whose many students of orbital mechanics included Mercury, Gemini, and Apollo astronauts.

REFERENCES

[1] Dichmann, D.J., Lebois, R. & Carrico, J.P. Dynamics of Orbits Near 3:1 Resonance in the Earth-Moon System. J of Astronaut Sci 60, 51–86 (2013).

[2] Dichmann, Donald & Parker, Joel & Nickel, Craig & Lutz, Stephen. (2016). Trajectory Design to Mitigate Risk for the Transiting Exoplanet Survey Satellite (TESS). 10.2514/6.2016-5664.

[3] Plice, Laura & Dono, Andres & Policastri, Lisa & Carrico, John & Loucks, Michel. (2018). Arcus Mission Design: Stable Lunar-Resonant High Earth Orbit for X-Ray Astronomy.

[4] West, Stephen & Carrico, John & Plice, Laura & Perez, Andres & Morrison-Fogel, Dylan & Levinson-Muth, Paul & Koehler, Andrew. (2020). Dynamics of Orbits near 4:1 Lunar Resonance.

[5] Plice L., Dono A., West S. "HelioSwarm: Swarm mission design in a highly elliptical orbit". AIAA/AAS Astrodynamics Specialists Conference, Portland, Maine, 2019.

[6] Gangestad, J. W., G. A. Henning, R. Persinger and G. R. Ricker, 2013. "A High Earth, Lunar Resonant Orbit for Lower Cost Space Science Missions". AAS 13-810.

[7] Dichmann, D., J. Parker, T. Williams, and C. Mendelsohn, "Trajectory Design for the Transiting Exoplanet Survey Satellite," International Symposium on Space Flight Dynamics, Laurel, MD, May 2014.

[8] Ely, T., "Stable Constellations of Frozen Elliptical Inclined Orbits," Journal of the Astronautical Sciences, Vol. 53, No. 3, July–Sept. 2005, pp. 301–316.

[9] Vallado, D. A., *Fundamentals of Astrodynamics and Applications*, 4th ed., Microcosm Press, Hawthorne, CA, 2013, Appendix D.3.

[10] Policastri, Lisa & Carrico, John & Lebois, Ryan. (2009). "Flight Dynamics Operations for the IBEX Mission: The First Six Months".

[11] Parker, J. J. K., R. L. Lebois, S. Lutz, C. Nickel, K. Ferrant, and A. Michaels, "Transiting Exoplanet Survey Satellite (TESS) Flight Dynamics Commissioning Results and Experiences," Paper No. 18-408, AAS/AIAA Astrodynamics Specialist Conference, Snowbird, UT, August 2018.